

Supporting Information

A Facile and Environmentally Friendly Route to Multiferroic Nanorods and Their Size-dependent Magnetic Properties

*Songping Wu ^{*a,b}, Yichao Lv ^a, Mingjia Lu ^a and Zhiqun Lin ^{*b}*

- a. School of Chemistry and Chemical Engineering, South China University of Technology, Guangzhou, 510641, China.
- b. School of Materials Science and Engineering, Georgia Institute of Technology, Atlanta, Georgia 30332, United States

*To whom correspondence should be addressed. E-mail: chwsp@scut.edu.cn. Fax & Tel: +86-20- 87112897; E-mail: zhiqun.lin@mse.gatech.edu. Tel: +1 404 385 4404.

Influence of pH on nanocrystals.

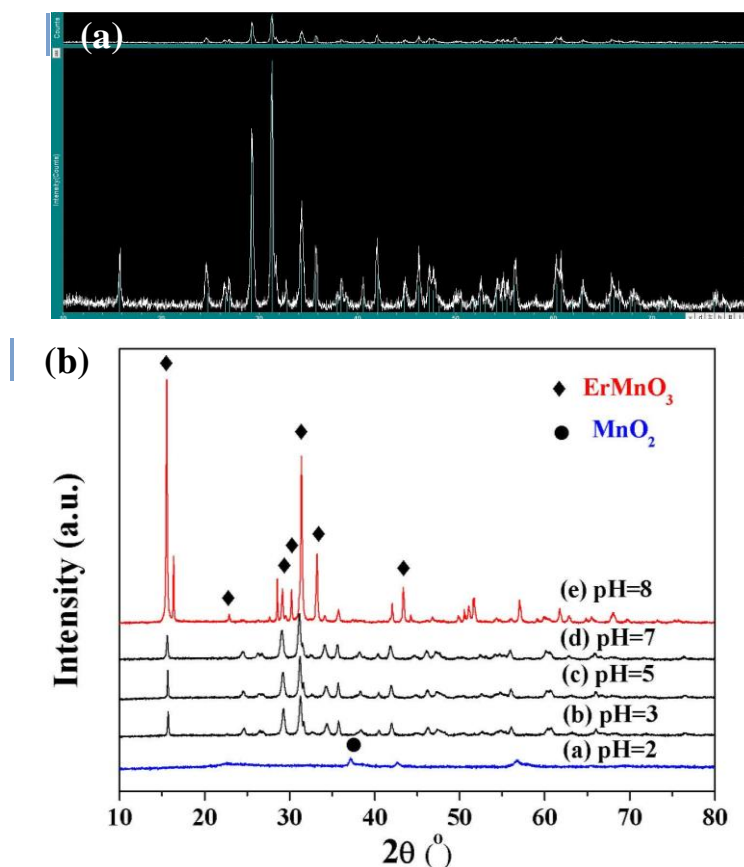


Figure S1. XRD profiles of samples synthesized under: (a) pH =3 at 250°C for 64 h (grey blue lines are the JCPDF lines), and (b) various pH values at 250°C for 64 h. (without the use of arabic gum as template)

FT-IR spectrum

Figure S2 depicts the FT-IR spectrum of ErMn_2O_5 nanorods. The absorption peaks at 443 cm^{-1} and 536 cm^{-1} can be ascribed to asymmetric stretching vibration of ErO_6 octahedron.¹ The absorption peak at 640 cm^{-1} corresponded to the Mn-O bending vibration.²

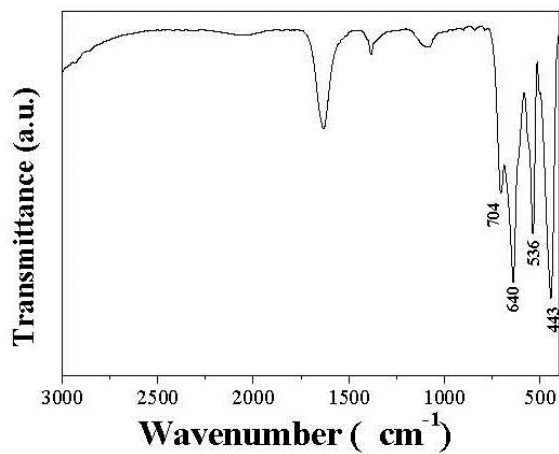


Figure S2. FT-IR spectrum of ErMn₂O₅ nanorods

Raman spectrum

Raman spectrum was acquired to investigate the local atomic structure of ErMn₂O₅ nanorods (**Figure S3**). The peaks at 218 cm⁻¹, 350 cm⁻¹, 465 cm⁻¹, 502 cm⁻¹, 630 cm⁻¹, and 705 cm⁻¹ can be assigned to A_g mode of orthorhombic ErMn₂O₅,³ and the peaks at 634 cm⁻¹ and 706 cm⁻¹ were ascribed to the stretching vibration modes of Mn-O.⁴ Notably, Raman spectroscopy is an extremely important tool to investigate antiferromagnetic transition temperature (T_N) and ferroelectric transition temperature (T_C) of RMn₂O₅.^{3,4}

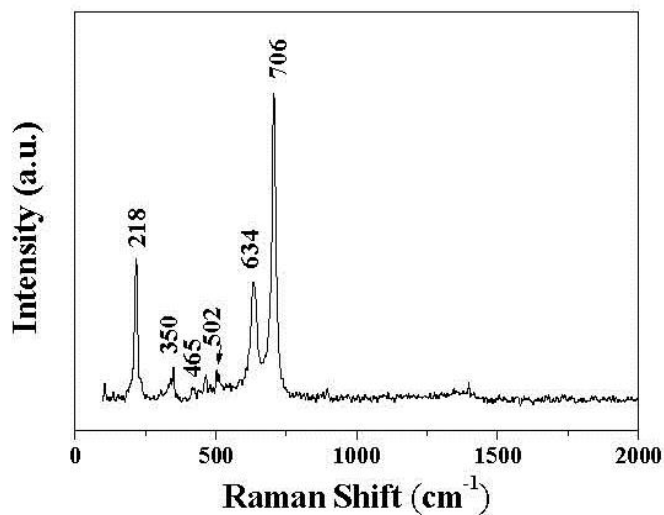


Figure S3. Raman spectrum of ErMn₂O₅ nanorods

UV-Vis spectra

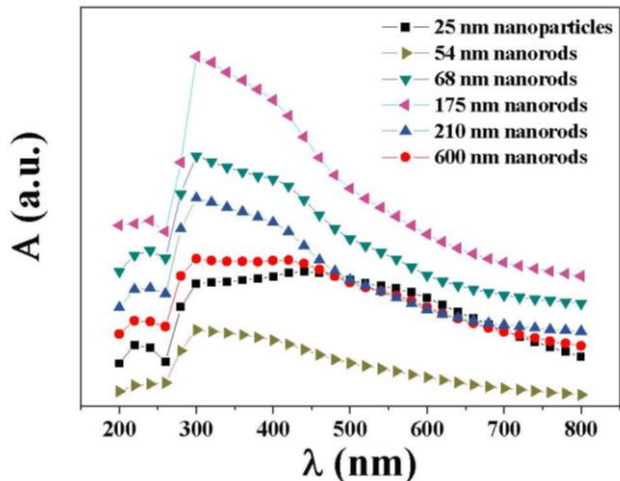


Figure S4. UV-Vis spectra of ErMn₂O₅ nanorods with various lengths at nearly constant diameter, $D = 28 \pm 3$ nm. For comparison, the nanorods with 600 nm in length and 60 nm in diameter were also measured (red curve). We note that the 25 nm nanocrystals were synthesized using manganese acetate as the divalent manganese source.

TGA/DSC analysis

TGA / DSC curves of ErMn₂O₅ samples were shown in **Figure S5**. As seen in the TGA curve, the total weight loss was approximately 4.42%, which can be divided into three stages.⁵ In the first phase (approximately 180 °C) about 0.6% weight loss was observed due to the volatilization of water in the sample. A weight loss of 0.7% can be attributed to the conversion of hydroxides of various metals to their oxides in the second stage (approximately 590°C). A significant 3.2% weight loss was found to occur at approximately 1020°C (the third stage), accompanying with a sharp endothermic peak at 1081.6°C in the DSC curve. As reported in the literature,⁶ thermal dissociation of ErMn₂O₅ follows three reaction stages over a temperature range of 973–1173 K (**Eqs. S1-S3**). Thus, it is reasonable to speculate that oxygen release contributes the weight loss at 1020°C for ErMn₂O₅.

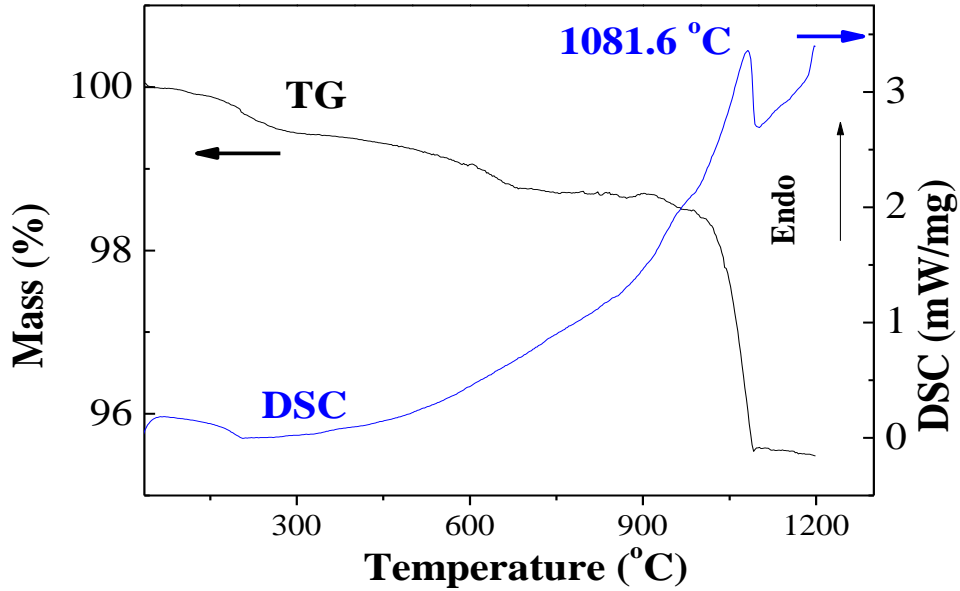
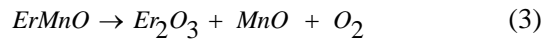
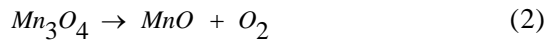
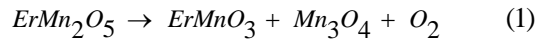


Figure S5. TGA/DSC curves of ErMn_2O_5 sample.



XRD profiles of nanorods at various amounts of arabic gum and pH values

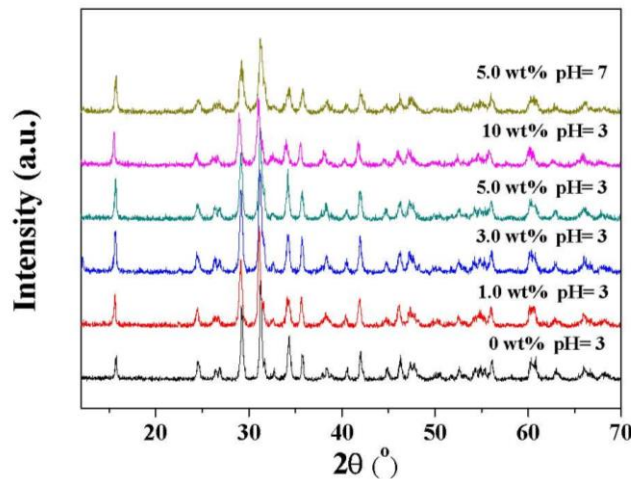


Figure S6. Representative XRD profiles of ErMn_2O_5 nanorods prepared using $\text{MnCl}_2 \cdot 4\text{H}_2\text{O}$ as the divalent manganese source with various amounts of arabic gum at different pH values.

Influence of the amount of arabic gum on morphology and length of nanorods.

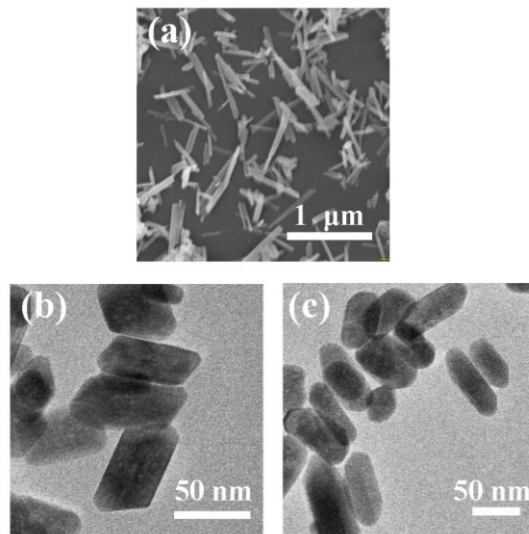


Figure S7. Typical SEM and TEM images of ErMn₂O₅ nanorods with various amounts of arabic gum at pH = 3: (a) 0 wt %; (b) 2 wt%, and (c) 5 wt%.

As shown in **Figure S8**, the length of ErMn₂O₅ nanorods at nearly constant diameter ($D=28 \pm 3$ nm) were 54 ± 5 nm, 68 ± 8 nm, 72 ± 7 nm, 125 ± 10 nm, 175 ± 25 nm, and 210 ± 30 nm, respectively, at the amounts of arabic gum of 2 wt%, 5 wt%, 6 wt%, 7.5 wt, 8 wt%, and 10 wt%, using MnCl₂·4H₂O as the divalent manganese source.

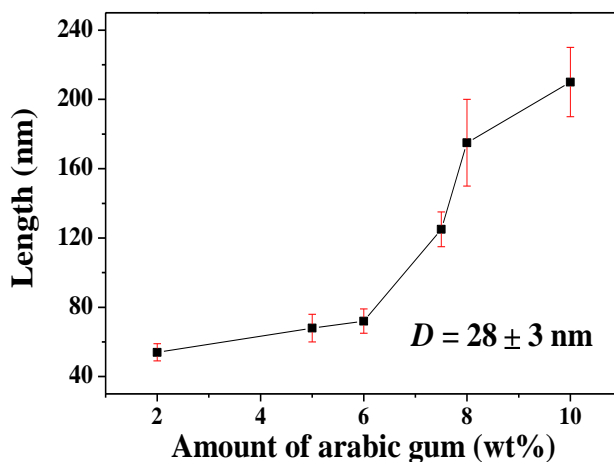


Figure S8. Influence of the amount of arabic gum on the length of nanorods

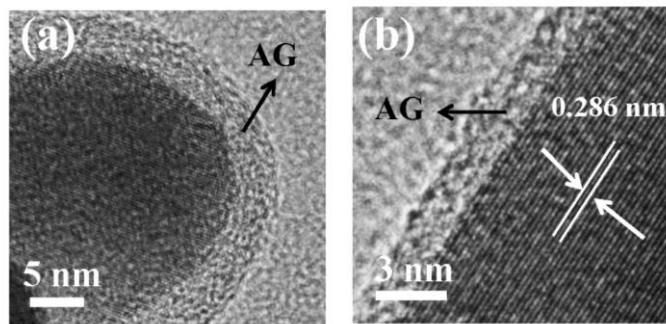


Figure S9. Typical HRTEM images of ErMn_2O_5 nanorods prepared with 10 wt% arabic gum at $\text{pH} = 3$.

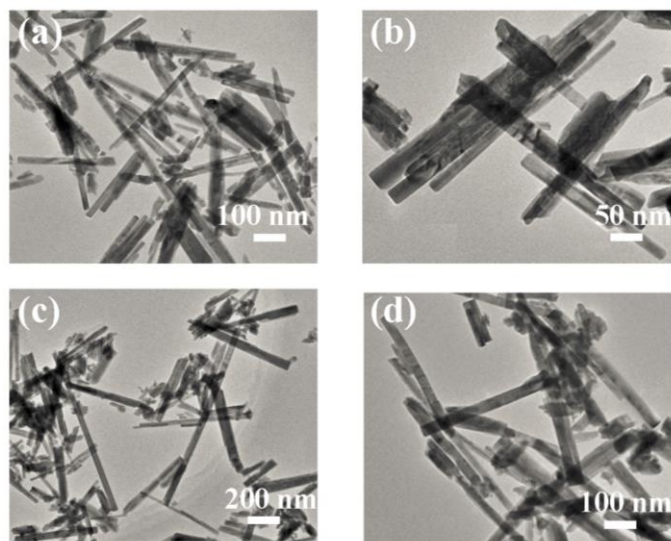


Figure S10. TEM images of ErMn_2O_5 nanorods formed with the large amount of arabic gum added: (a, b) 12 wt% arabic gum, and (c, d) 14 wt% arabic gum.

The surface to volume ratio for nanorods.

For single-domain antiferromagnetic nanorods, the magnetization is expected to scale as $\sim (1/L + 2/D)$ (i.e., the surface to volume ratio), where L is the length of nanorods, and D is the diameter of nanorods (i.e. 28 ± 3 nm).^{7, 8}

For spherical nanoparticles or nanorods, the ratio of surface to volume can be calculated according to the **Eqs. S4 and S5**, respectively.

$$\frac{S_{sphere}}{V_{sphere}} = \frac{4\pi(D_s/2)^2}{4\pi(D_s/2)^3/3} = \frac{6}{D_s} \quad (4)$$

$$\frac{S_{rod}}{V_{rod}} = \frac{2\pi(D_r/2)^2 + \pi dL}{\pi(D_r/2)^2 L} = \frac{2}{L} + \frac{4}{D_r} \quad (5)$$

where S and V are the surface area and the volume of nanoparticles or nanorods, respectively; D_s is the diameter of nanoparticles, D_r is the diameter of nanorods, and L is the length of nanorods. We assume that the same ratio of surface to volume exerts the equal influence on the magnetic properties, regardless of their morphologies (nanoparticles or nanorods), so the ErMn_2O_5 nanorods (varied length and nearly constant diameter) can be regarded as an equivalent nanoparticles. The equivalent diameters are summarized in **Table S1**. Obviously, the equivalent diameters for ErMn_2O_5 nanorods are in the region of 26.9 ~ 85.7 nm. Thus, we believe that a linear dependence of magnetization on the size of BiFeO_3 nanoparticles (with the nanoparticle diameter ranging from 41 to 95 nm) reported in literature⁸ may be observed in the present study, as our equivalent diameters fall in the range of 26.9 ~ 85.7 nm.

Table S1. Equivalent diameters of nanorods calculated based on Eqs. S4 and S5

L (nm)	600	210	175	125	68	54	25
D (nm)	60	28 ± 3					
Equivalent diameter (nm)	85.7	39.4	38.9	37.8	34.8	33.4	26.9

Magnetic properties at low temperature.

Table S2. Derived magnetic properties at 20 kOe at 10K^a

L (nm)	$1/L(\text{nm}^{-1})$ ($\times 100$)	M_s (emu/g)	θ_{cw} (K)	H_c (oe)	μ_{eff} (μB)	M_r (emu/g)	M_r/M_s ($\times 10^4$)
25	4	33.64	-16.23	8.75	10.44	0.015	4
68	1.47	35.97	-16.8	19.05	10.59	0.024	6.67
125	0.8	36.13	-16.24	17.15	10.57	0.029	8
175	0.57	37.74	-17.6	16	10.81	0.029	7.68
210	0.48	36.57	-16.56	18.5	10.6	0.032	8.75
600*	0.16	34.2	-19.6	17.2	10.46	0.03	8.77

L is length of ErMn_2O_5 ($D = 28 \pm 3$ nm). M_s is the magnetization observed at $H = 20$ kOe. The magnetic moments are defined in units of emu/g. H_c , μ_{eff} and M_r represent derived coercivities, effective paramagnetic moments and remnant magnetization, respectively. * $D = 60$ nm.

Temperature dependence of magnetization for ErMn_2O_5 nanorods

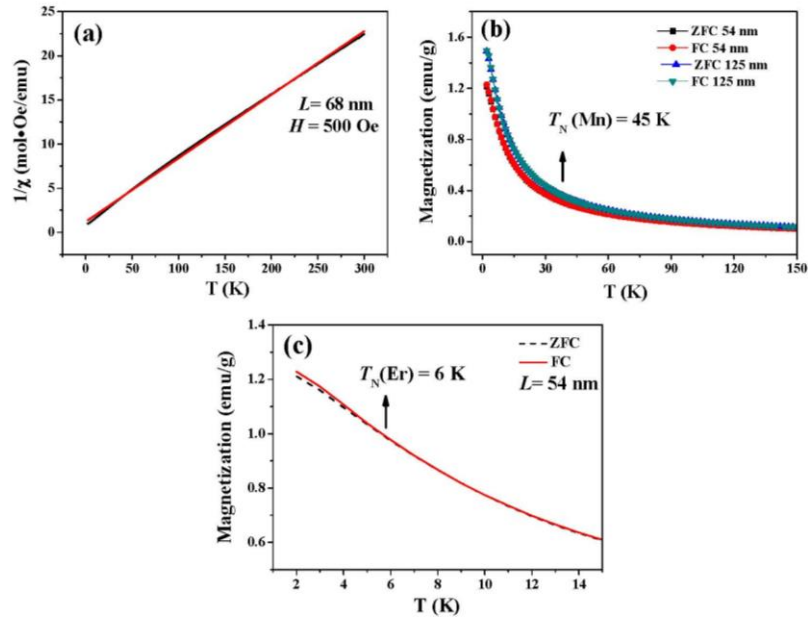


Figure S11. (a) Typical inverse magnetic susceptibility of ErMn_2O_5 nanorods at a magnetic field of $H = 500$ Oe over a temperature range from 2 to 300 K. The red line is the Curie–Weiss fitting. (b) Temperature dependence of magnetization for ErMn_2O_5 nanorods with various lengths, showing zero field cooling (ZFC) and field cooling (FC) curves, at an applied magnetic field, $H = 500$ Oe. (c) Expanded plots of ZFC and FC curves for ErMn_2O_5 nanorods with L of 54 nm and D of 28 nm.

Effect of arabic gum on magnetic properties

To highlight the influence of arabic gum on the magnetic property of templated ErMn_2O_5 nanorods, the ErMn_2O_5 nanorods ($L = 210 \text{ nm}$) were annealed at $500 \text{ }^\circ\text{C}$ for 30 minutes to remove arabic gum on their surface. The result showed that the template-free specimen possessed larger M_r and M_s values (**Figure S12a,b**) and a high divagation temperature ($\sim 53 \text{ K}$) (**Figure S12c**). Obviously, the surfactant (i.e. Arabic gum) exerts a subtle influence on the magnetic behaviour of resultant nanorods. Such a phenomenon was also observed in the CTAB, which really changed the magnetic behaviors of CuGeO_3 nanobelts.⁹

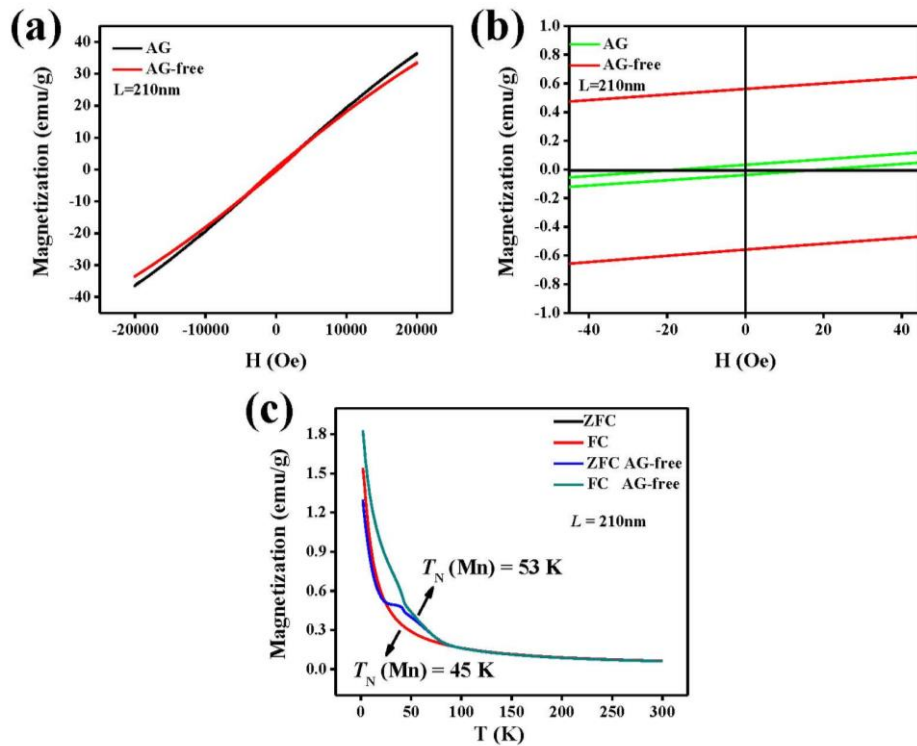


Figure S12. (a) Magnetic properties of ErMn_2O_5 nanorods at length of 210 nm measured at 10 K , showing the hysteresis loops. The nanorods were prepared by capitalizing on arabic gum as template. For comparison, the hysteresis loop of AG-free nanorods, whose arabic gum templates were destroyed at 500°C for 30 minutes, was also measured. (b) The magnetizations of ErMn_2O_5

nanorods with L of 210 nm and AG-free ErMn_2O_5 , respectively, from $H = -50$ to 50 Oe. (c) Temperature dependent magnetization of ErMn_2O_5 nanorods (length of 210 nm) and AG-free ErMn_2O_5 , showing zero field cooling (ZFC) and field cooling (FC) curves at magnetic field, $H = 500$ Oe.

References

1. X. M. Cao, Z. M. Lu and J. H. Chen, *J. Rare Earths*, 2007, 25, 207-210.
2. G. V. Chertihin and L. Andrews, *J. Phys. Chem. A*, 1997, 101, 8547-8553.
3. B. Mihailova, M. M. Gospodinov, B. Güttler, F. Yen, A. P. Litvinchuk and M. N. Iliev, *Phys. Rev. B*, 2005, 71, 172301.
4. A. F. García-Flores, E. Granado, H. Martinho, R. R. Urbano, C. Rettori, E. I. Golovenchits, V. A. Sanina, S. B. Oseroff, S. Park and S. W. Cheong, *Phys. Rev. B*, 2006, 73, 104411.
5. A. Mahmood, M. F. Warsi, M. N. Ashiq and M. Sher, *Mater. Res. Bull.*, 2012, 47, 4197-4202.
6. L. B. Vedmid', V. F. Balakirev, A. M. Yankin, Y. V. Golikov and O. M. Fedorova, *Inorg Mater*, 2008, 44, 316-318.
7. T. Kimura, G. Lawes, T. Goto, Y. Tokura and A. P. Ramirez, *Phys. Rev. B*, 2005, 71, 224425.
8. T. Park, G. C. Papaefthymiou, A. J. Viescas, A. R. Moodenbaugh and S. S. Wong, *Nano Lett.*, 2007, 7, 766-772.
9. R.-Q. Song, A.-W. Xu and S.-H. Yu, *J. Am. Chem.Soc.*, 2007, 129, 4152-4153.